

Static Structural Analysis of a Variable Span Morphing Wing for Unmanned Aerial Vehicle

M Bashir and P Rajendran

School of Aerospace Engineering, Universiti Sains Malaysia, Engineering Campus,
Nibong Tebal, Pulau Pinang, Malaysia.

Email: aeparvathy@usm.my

Abstract. While the primary reason to develop an adaptive wing is the aerodynamic benefits, the primary hindrance is the structural and vibrational considerations due to the unsteady nature of the airflow during the flight. Hence this study forms an important part of the morphable wing technology. In this paper, the design of a moderate aspect ratio variable span wing will be performed. The morphing wing is modeled structurally to observe the effect of spanwise load distribution on the wing structure. For the structural design and analysis of the unmanned aerial vehicle (UAV) under this study, commercial software Solidworks and Ansys/Static Structural/Modal are used. The static structural analyses of the wing are performed under different load conditions. The results of these analyses show that the designed structure is safe within the flight envelope. It is observed that the wing-root bending moment increases drastically due to an increase in the wingspan. Thus, the bending moment along the wingspan of the morphing wing is much larger than that of the conventional wing which results in an increase in the deflection of the free-end. The maximum stress for the un-extended wing configuration increases for the extended wing configuration.

1. Introduction

Capability of changing the wing during flight can be referred to “Morphing”. This capability may result in economical fuel consumption, increase in mission adaptability and performance. Fixed wing aircraft are designed for considering the flight envelope and the mission profiles. For instance, fixed wing aircraft which are designed for high altitude level flight is not suitable for a dog fight. The aim of a morphing wing is the ability to adapt the wing for a variety mission phases.

Morphing wings coupled with the availability of light-weight, high-strength materials over the last couple of decades; have exhibit increase in aerodynamic efficiency with increasing aspect ratio. For instance a study has shown the efficiency of high altitude long endurance configurations also increases with increasing wing aspect-ratio and decreasing structural weight [1]. However, the resulting structure exhibits low structural stiffness, leading to significant static aeroelastic deformations at the tip of extended sections.

Several studies have been conducted on using composite materials for the design of aircraft wing. Newman Iii et al [2] demonstrated a computationally efficient with high-fidelity and integrated static aeroelastic analysis procedure. Here, the aerodynamic analysis consists of solving the nonlinear Euler equations by using an upwind cell-centered finite-volume scheme on unstructured tetrahedral meshes.



They presented static aeroelastic analysis results for a flexible wing in low subsonic, high subsonic (subcritical), transonic (supercritical), and supersonic flow conditions.

Bae et al [3] presented aerodynamic and aeroelastic analysis of variable span morphing wing (VSMW). The aeroelastic analysis shows that the flexibility of morphing wing structure increases as the wing span increases. At a given flight condition, the aerodynamic deformation is much larger than that of the conventional wing. Static aeroelastic considerations show that a VSMW requires increased bending stiffness because the wing deformation due to bending is much more significant than the deformation due to twist, which demands that VSMW designers include larger bending stiffness in their formulation.

Also, Santos et al [4] developed a fully functional VSMW system covering areas from aerodynamic optimization and structural design, through prototyping and flight testing. The results showed that both deployment and load tests revealed satisfactory performance for VSMW concept. However, deployment can be improved by increasing the skin stiffness at the inboard fixed wing tip with an internal stiff rib (between sandwich facings). Or else, this can also be achieved using an external lighter rib similar to an end plate around the perimeter of the airfoil.

Andersen et al [5] utilized an evolutionary process to analyze and characterize the dynamic aeroelastic features. It was concluded that NextGen's experience gained during the flutter prediction efforts indicated significant opportunities for aeroelastic modeling and analysis method developments. Aeroelastic characterization of morphing aircraft structures would benefit from both advances in automated structure, aerodynamic, and spline modeling. Elham [6] concluded that using composite materials in designing a wing box will reduce the weight up to 40% compared to aluminum wing box.

Potter et al [7] also investigated the physics-based structural analysis and also found that the optimal rib-spacing in a wing box should be optimized, and the use of composite materials reduced the weight up to 30% compared to the aluminum one. Gürses et al [8] studied the structural design to increase and decrease the camber control surface to match selected airfoil profiles. Schorsch et al [9] developed an elastomer based skin for seamless morphing of a rib based adaptive trailing edge. The skin material development focused on low temperature requirements for cruise flight conditions, resistance to environmental conditions as well as long fatigue life.

Xu [10] focused on the effect of wing skin thickness on the stiffness and strength of a composite wing. Recently, Naidu and Adali [11] designed a wing box structure for Medium Altitude Long Endurance UAV. However, they only considered a sandwich structure, using isotropic and composite materials. Pecora et al [12] worked on the design process to enable the high-fidelity reproduction of target shapes under the action of aerodynamic and inertial loads; and avoid any detrimental impact on flight safety as well as on the overall aircraft maintenance plans.

2. Methodology

The wing baseline geometry in this paper is similar to Phoenix UAV wing that has a moderate aspect ratio UAV. Nevertheless, the methodology presented in this paper can be used to design any arbitrary aircraft wing having moderate aspect ratio. Since we are employing VSMW, the area under the lift distribution is equal to the total lift produced by the morphing wing. When the aircraft would undergo the telescopic extension and increase the wingspan from 1.2 m to 1.8 m, it would achieve a higher aspect ratio. Keeping the chord lengths constant, but increasing the span to 0.6 m we see an increase in the aspect ratio. Additionally, the wing is considered rectangular because the chord of extended section is nearly equal to the chord of fixed wing profile.

Since the internal structure of the given UAV wing was unknown, the current structure was designed according to the standard wing structural design. The current structure consists of 3 main components: 10 ribs (6 in fixed wing part with 10 cm rib spacing, and 4 in extended part with 15 cm spacing), 2 spars at 25% and 75% wing chord, and skin panels. The rib spacing was chosen to have the maximum buckling strength of the panels, while the spars position was chosen to accommodate the maximum torsional stiffness according to the design practices in the wing structural design. Summary of the wing geometry specification is shown in Table 1.

Table 1. Wing Geometry Specification.

Wing Feature	Value
Wing Semi-Span WOE	1.2 m
Wing Semi-Span WE	1.8 m
Fully Extended Wing Area	0.36 m ²
Aspect Ratio	9
Chord	0.2 m
Airfoil	NACA 0018

2.1 Load Analysis of Wing

A static finite element method was used extensively during the design processes. In this study, the moderate-aspect-ratio VSMW is investigated. Lift load is considered as important criteria while designing an aircraft. Fuselage and wing are the two main regions where lift load acting in an aircraft. Here 80% of the lift load is acted on the wings (i.e., maximum lift load is acted on the wings) and remaining 20% in acted on the fuselage. Therefore in wings the maximum load is acted nearer to the wing roots.

Equation 1 below estimates lift, L produced by UAV where n is design load factor and W is the weight of UAV. Table 2 below summarizes the calculated features of investigated wing similar to Phoenix UAV. Considering the weight of the aircraft, design load factor, and factor of safety, the total design load of UAV can be estimated. This force is converted into the pressure load as uniformly distributed load by dividing this force for the semi wing area of 0.4 m². Therefore, the total pressure load applied from the bottom of the surface is 200 Pa.

$$L = n \times W \quad (1)$$

Table 2. Summarizes the calculated features of investigated wing.

Details	Calculated Value
Weight of UAV	500N
Design Load Factor	3g
Factor of Safety	1.5
Total Design Load	450 N
Total Lift Load on Fuselage (20%)	50 N
Total Lift Load on Wings (80%)	400N

2.2 Modelling and Grid Generation

The solid modeling of the airfoil was made with the help of Solidworks 16.0 as shown in Figure 1. The materials and their sectional properties of wing components are presented in Table 3. In addition, mechanical properties of an isotropic material, Aluminum 2024-T3 used in the Ansys Engineering model has been presented in Table 4.

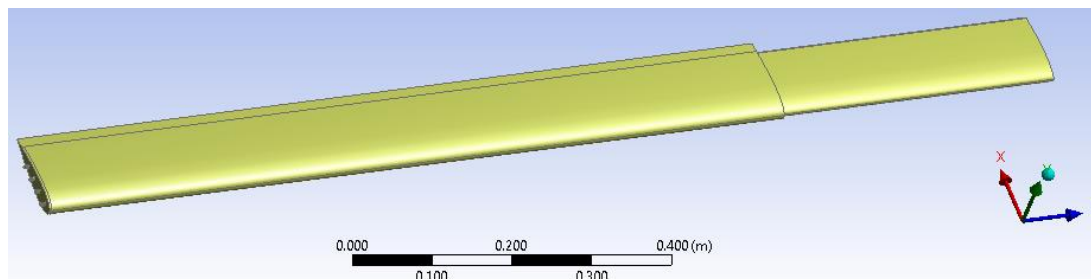
**Figure 1.** The solid modeling of the airfoil.

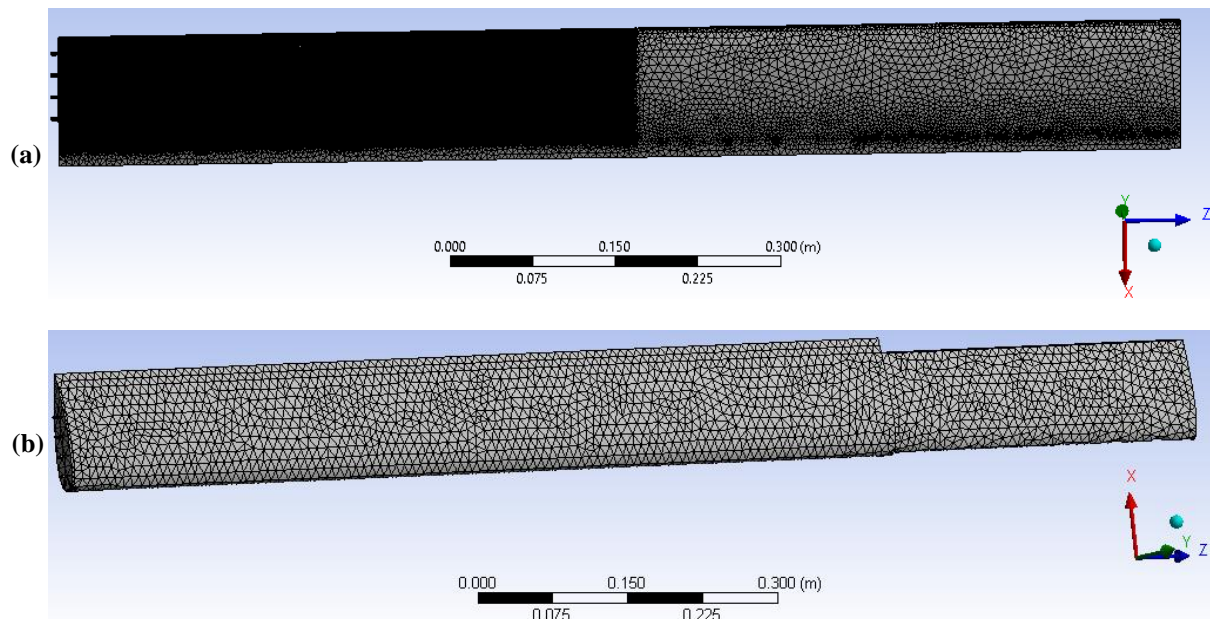
Table 3. Materials and their sectional properties of wing components.

Element Property	Material	Thickness (mm)
Spar Webs	Structural Steel	2.54
Ribs	Structural Steel	0.80
Aluminium Skin	Aluminium 2024-T3	1.50

Table 4. Properties of Aluminium 2024-T3.

Property	Value
Density	2780 kg/m ³
Young's Modulus, E	73.1 GPa
Shear Modulus, G	28.0 GPa
Poisson's Ratio, ν	0.33
Ultimate Strength	483 MPa
Yield Strength	385 MPa
Shear Strength	283 MPa

The unstructured mesh has been generated for CFD static structural analysis of the moderate-aspect-ratio wing model. Unstructured meshes are usually flexible because they conform to intricate shapes easily but they have drawback for treating the viscous boundary layer region. The wing meshes for both un-extended and extended span are shown in Figure 2.

**Figure 2.** Wing meshes for both (a) un-extended and (b) extended span.

3. Results and Discussion

After the generation of pressure boundary condition, the wing is fixed from its one end and then the static analysis is performed. The result is given as deformation of the wing in model scale along with Von Mises stress and strain plots. The boundary conditions to analyse the wing conditions are developed by creating pressure load on the lower surfaces of wing. Based on the Equation 1, pressure load value of 200 Pa has been estimated. The five different cases shown in Figure 3 are analysed one by one analysed based upon the span change and applied load conditions is given in the following subsections.

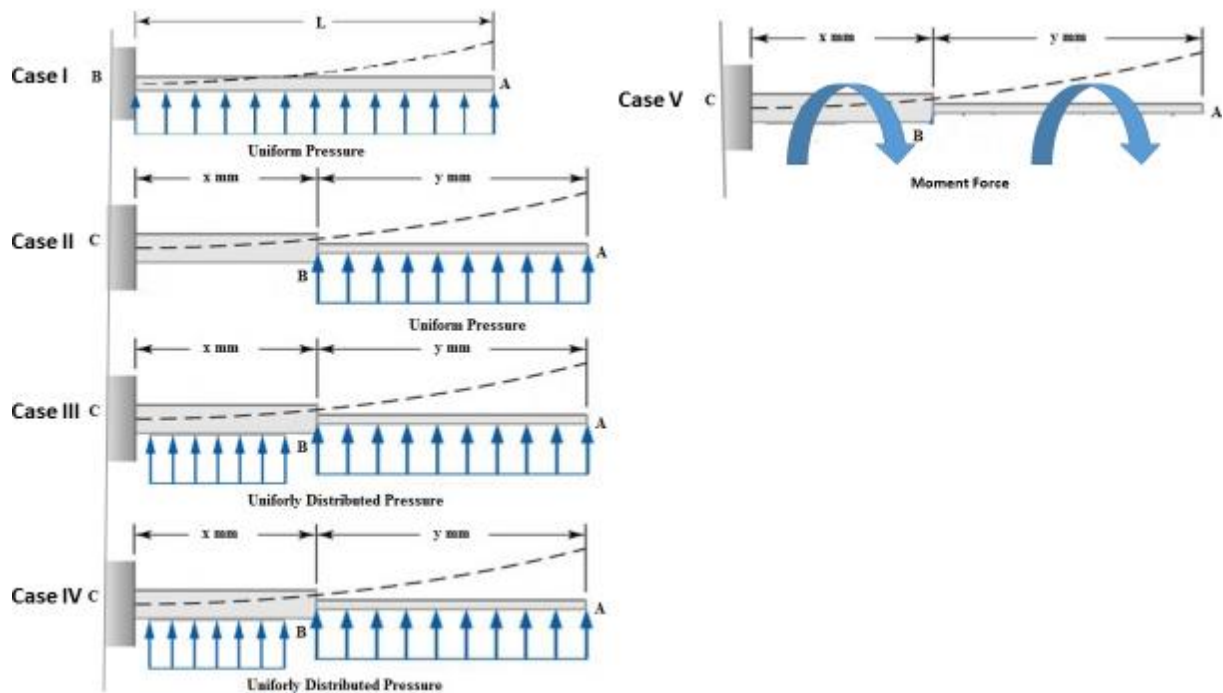


Figure 3. The five case studies based on the span change and applied load condition.

3.1 Case I - Without Extension

Figure 4 depicts the deformation of the un-extended wing along with stress and strain values. From the figure, it is so clear that the tip of the wing under goes maximum deformation and the root region is under tremendous stress, but it is still under control. The maximum deformation value shows 8.7375×10^{-5} and also the stresses are below the allowable the value. It is clear that the structure is safe enough to take the loads. This structure is safe enough to withstand this particular manoeuvring with enough factor of safety.

3.2 Case II - With Extension but load on extended Part only

In this case, the pressure is applied on the extended section only. Figure 5 shows the total deformation, Von Mises stress, and Equivalent strain. It is seen that maximum deflection occurs at the tip of extended wing, and the material starts to yield when the Von Mises stress reaches a critical value, yield strength. The stress distribution for the given loads has been observed. Here, the stress is distributed uniformly but maximum stresses are developed nearer to root of wing section. In this case, the Von Mises stress observed in the wing analysis is 72 MPa. The Yield strength of the aluminium alloy AA 2024-T3 is 385 MPa. Thus, the structure is safe because the stress magnitude which was obtained from the analysis is less than the yield strength of the structural material.

3.3 Case III - With Extension but uniformly distributed load over the wing surface

Figure 6 depicts the case of static analysis of the span extended wing with uniformly distributed pressure performed using ANSYS Workbench. As expected, it shows that the maximum deflection increases from 0.00087375 m for the un-extended wing case to 0.0082961 m for the case of telescopic extension of the wing with uniformly distributed pressure throughout the wing. From the figures it is so clear that the root region is under tremendous stress, but it is still under control. The maximum stress value shows 3.8669×10^7 Pa and still within the allowable value. It is clear that the structure is safe enough to take the loads.

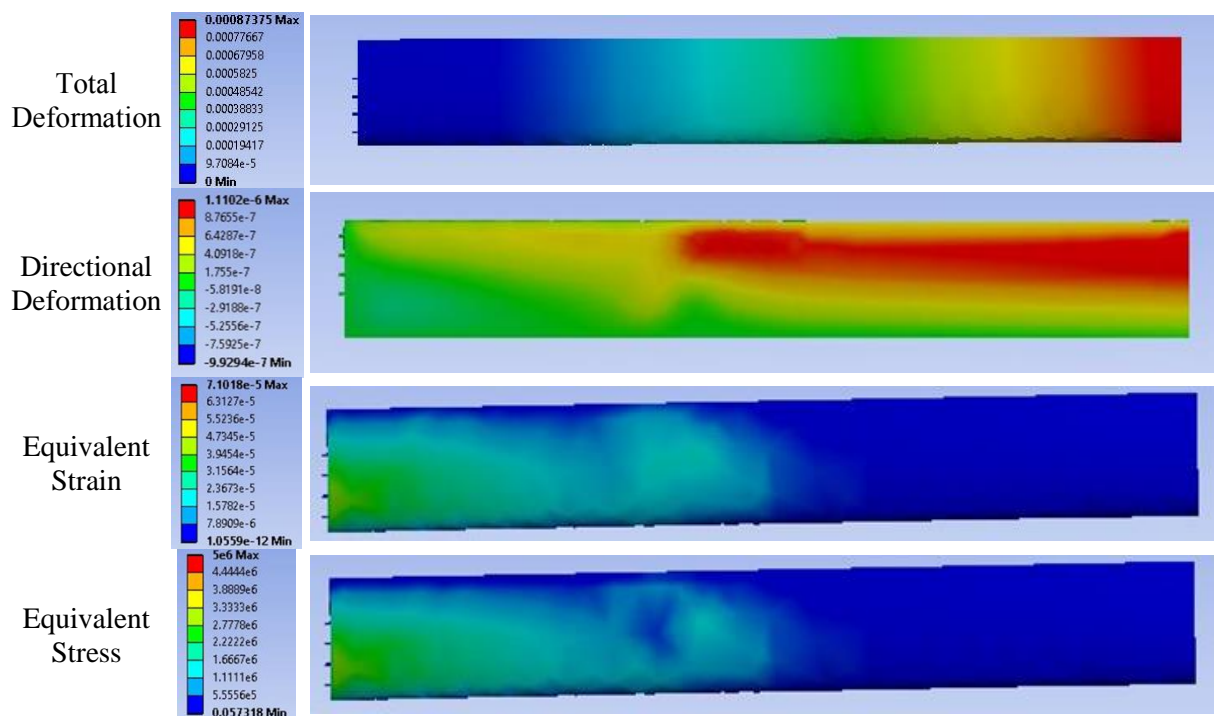


Figure 4. Case I - Without Extension

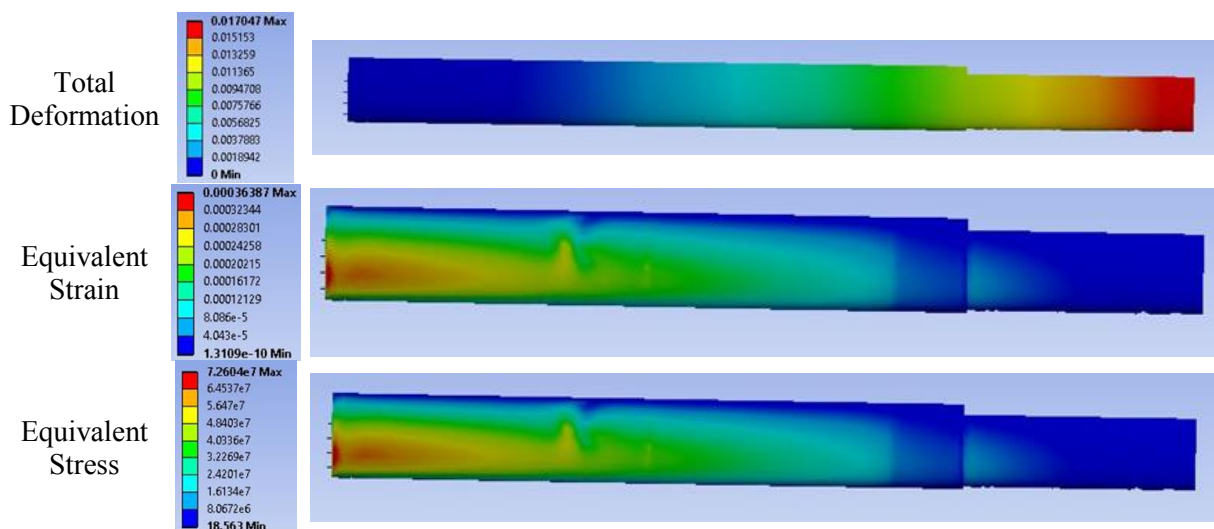


Figure 5. Case II - With Extension but load on extended Part only

3.4 Case IV – Modal analysis of Wing

In order to determine the effects of inertial loads during manoeuvres and natural frequencies, modal analysis was also performed. Modal analysis comprises of deformation calculations due to loads at higher load factors and estimation of natural frequencies and mode shapes. The mode shapes for corresponding frequencies are given in Figure 7.

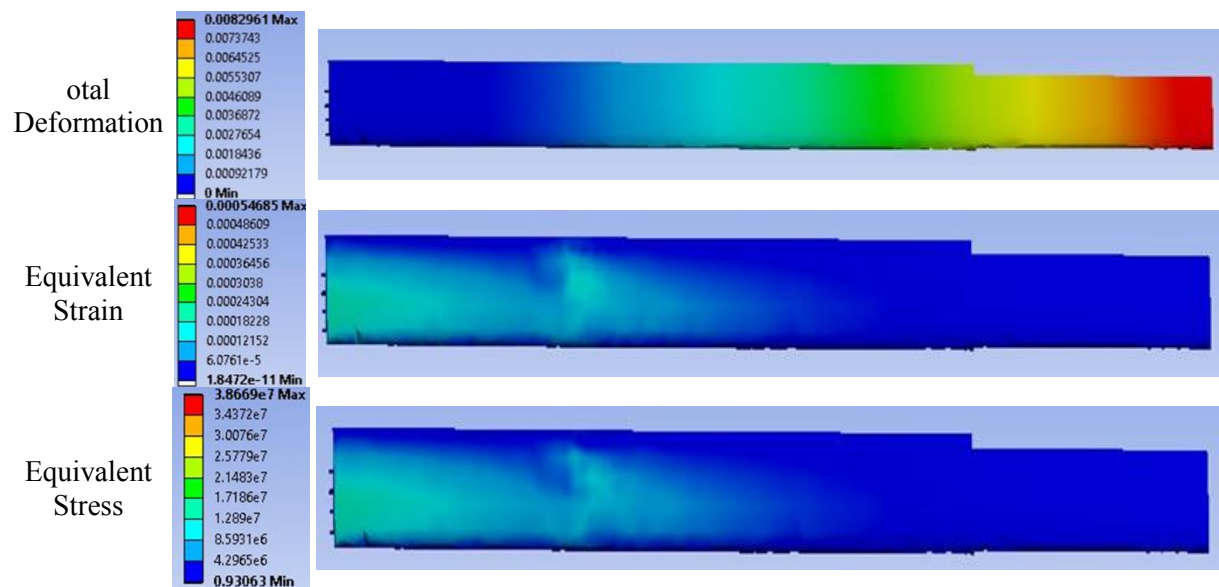


Figure 6. Case III - With Extension but uniformly distributed load over the wing surface

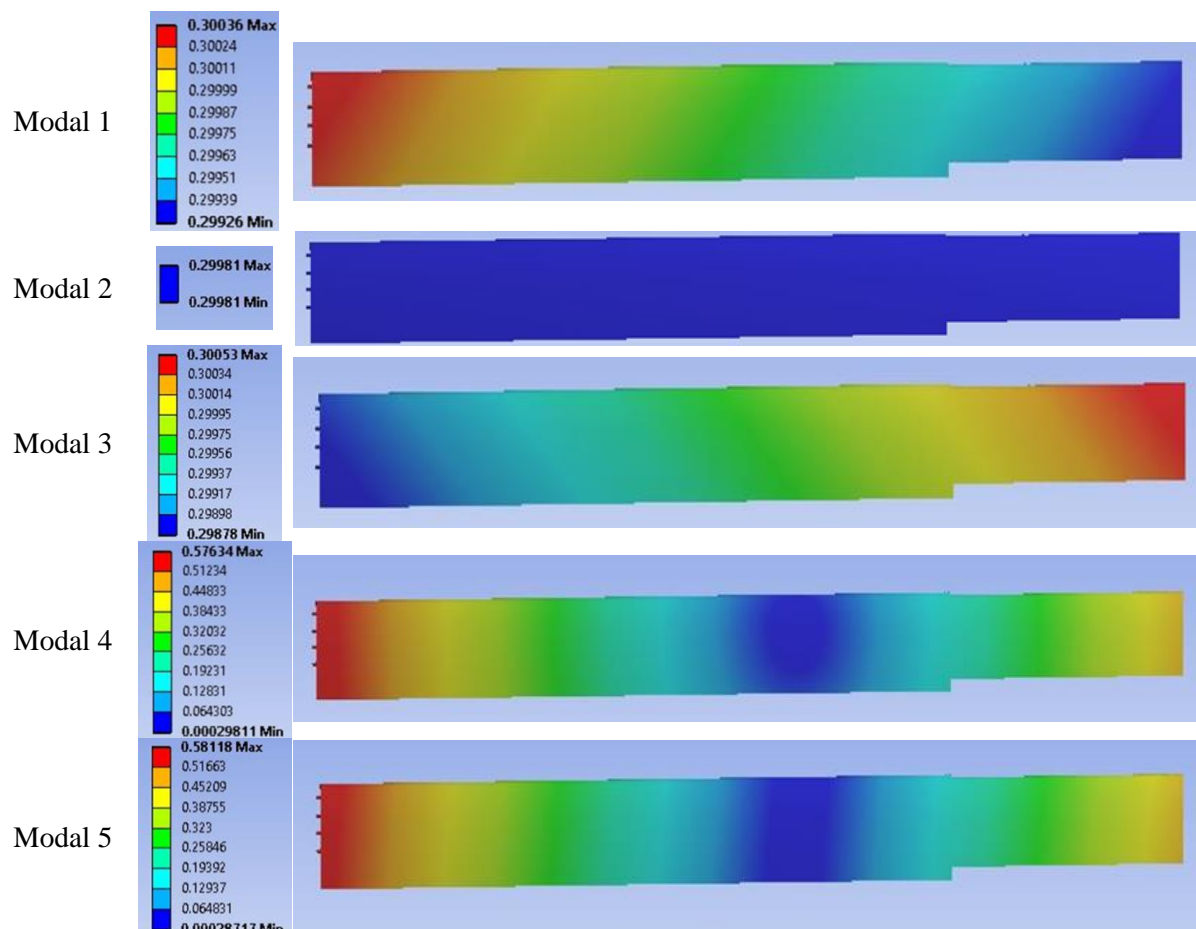


Figure 7. Case IV – Modal analysis of Wing

3.5 Case V - Application of Moment Force over the Leading Edge of Wing

Figure 8 shows that the wing-root bending moment increases drastically due to an increase in the wingspan. Thus, the bending moment along the wingspan of the morphing wing is much larger than that of the conventional wing which results in an increase in the deflection of the free-end. The maximum stress for the un-extended wing configuration increases for the extended wing configuration.

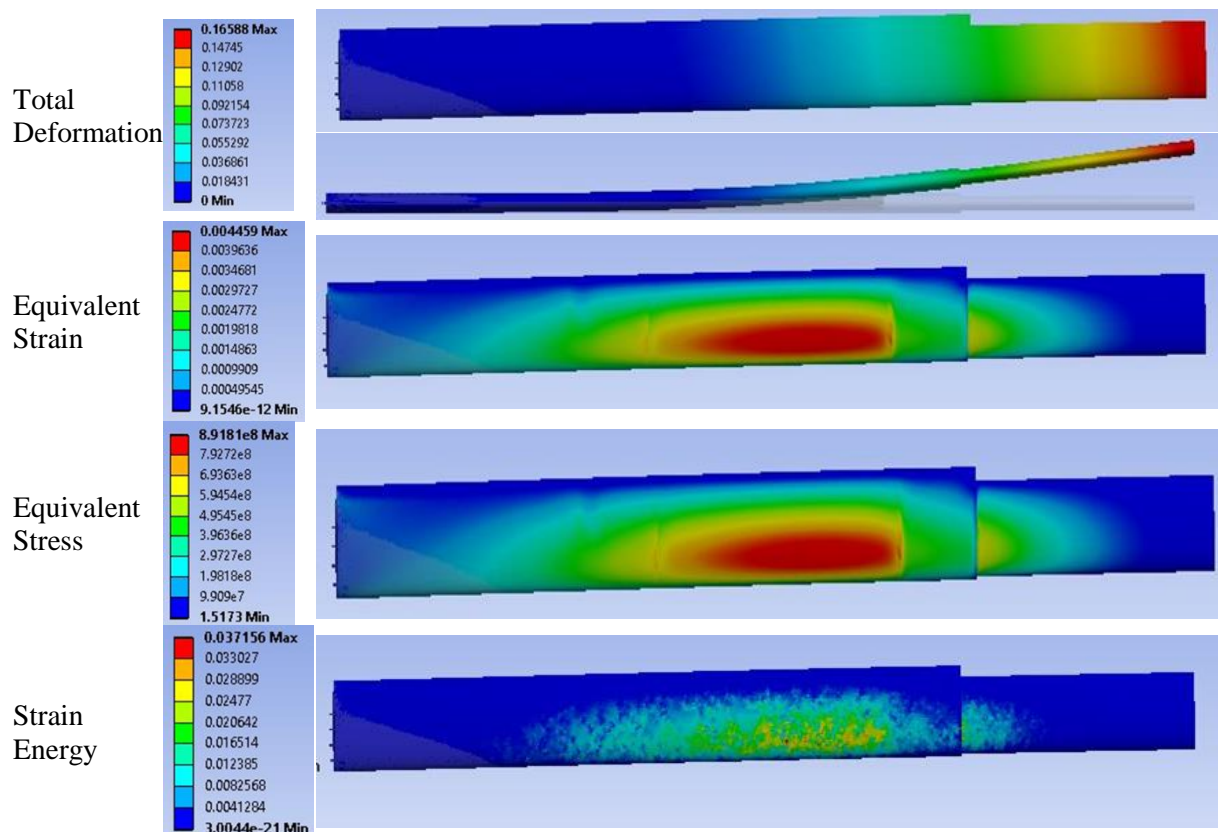


Figure 8. Case V of Moment Force over the Leading Edge.

4. Conclusion

Morphing UAV wing model as per the design considerations is developed in Solidworks and the model is imported into Ansys/Static Structural and subjected to various loading. The loading are calculated according to the aerodynamic lift load analysis by considering various design factors and the deflection over have been estimated. As seen in the results, the wing is severely affected by the loads on extended part, and the deflection is maximum at the tip of extended section. Moreover, the moment loading applied in one case shows the deflection increases further by the moment force. Also, the stress and strain values increased at the hinged joints between two wing sections. Von misses stress is calculated in order to know the maximum stress levels and minimum stress levels on the wing. Their differences are shown clearly with the contour stress levels. The deflection and stress levels are shown from minimum to maximum in the color contours. Their values are given side by side. The wing structure has been optimally analyzed which satisfies the strength and stability criteria.

Acknowledgement

This publication was supported by Universiti Sains Malaysia Grant No. 304/PAERO/6315002.

References

- [1] M. J. Patil, D. H. Hodges, and C. E. Cesnik, "Nonlinear aeroelasticity and flight dynamics of high-altitude long-endurance aircraft," *Journal of Aircraft*, vol. 38, pp. 88-94, 2001.
- [2] J. N. Iii, P. Newman, A. T. Iii, and G.-W. Hou, "Efficient nonlinear static aeroelastic wing analysis," *Computers & fluids*, vol. 28, pp. 615-628, 1999.
- [3] J.-S. Bae, T. M. Seigler, and D. J. Inman, "Aerodynamic and static aeroelastic characteristics of a variable-span morphing wing," *Journal of aircraft*, vol. 42, pp. 528-534, 2005.
- [4] P. Santos, J. Sousa, and P. Gamboa, "Variable-span wing development for improved flight performance," *Journal of Intelligent Material Systems and Structures*, vol. 28, pp. 961-978, 2017.
- [5] G. R. Andersen, D. L. Cowan, and D. J. Piatak, "Aeroelastic modeling, analysis and testing of a morphing wing structure," in *Proceedings of 48th AIAA/ASME/ASCE/AHS/ASC structures, structural dynamics and materials conference*, 2007, pp. 23-26.
- [6] A. Elham, "Effect of wing-box structure on the optimum wing outer shape," *The Aeronautical Journal*, vol. 118, pp. 1-30, 2014.
- [7] C. L. Potter, S. G. Russell, V. Kim, Z. Liu, and D. N. Mavris, "Design Space Exploration of Wing Box Substructures Configuration Using SPANDSET," in *16th AIAA/ISSMO Multidisciplinary Analysis and Optimization Conference*, 2015, p. 2789.
- [8] E. Gürses, İ. O. Tunçöz, Y. Yang, P. Arslan, U. Kalkan, H. Tıraş, M. Şahin, S. Özgen, and Y. Yaman, "Structural and aerodynamic analyses of a hybrid trailing edge control surface of a fully morphing wing," *Journal of Intelligent Material Systems and Structures*, vol. 28, pp. 979-991, 2017.
- [9] O. Schorsch, A. Lühring, C. Nagel, R. Pecora, and I. Dimino, "Polymer based morphing skin for adaptive wings," in *Proceedings of the 7th ECCOMAS thematic conference on smart structures and materials (SMART 2015), Ponta Delgada, Azores, submitted*, 2015.
- [10] R. Xu, "Optimal design of a composite wing structure for a flying-wing aircraft subject to multi-constraint," 2012.
- [11] Y. Naidu and S. Adali, "Design and Optimization of a Medium Altitude Long Endurance UAV Wingbox Structure," *R & D Journal of the South African Institution of Mechanical Engineering*, vol. 30, pp. 22-29, 2014.
- [12] R. Pecora, I. Dimino, F. Amoroso, and M. Ciminello, "Structural design of an adaptive wing trailing edge for enhanced cruise performances," in *Proceedings of 24th AIAA/AHS Adaptive Structures Conference. San Diego*, 2016.